



Ab Initio Study of TEPA Adsorption on Pristine, Al and Si Doped Carbon and Boron Nitride Nanotubes

Mir Saleh Hoseininezhad-Namin^{1,2} · Parinaz Pargolghasemi³ · Maryam Saadi³ ·
Mohammad Ramezani Taghartapeh⁴ · Nafiseh Abdolahi⁵ · Alireza Soltani⁵ · Andrew Ng Kay Lup⁶

Received: 25 February 2020 / Revised: 13 July 2020 / Accepted: 15 July 2020
© Springer Science+Business Media, LLC, part of Springer Nature 2020

Abstract

The present first principles study entails the adsorption behavior of N, N', N''-triethylenephosphoramidate (TEPA) drug over the pristine, Si- and Al-doped (5, 5) armchair single-wall carbon and boron-nitride nanotubes (SWCNTs and SWBNNTs). Density functional theory (DFT) calculations were done via the B3LYP and M06-2X methods with the standard 6-31G** basis set. The results show that the adsorption of TEPA drug molecule occurred physically on pristine CNT and BNNT and chemically on Al- and Si-doped CNTs and BNNTs. Although Si- and Al-doped CNTs and Al-doped BNNT provide stronger adsorption, the change in the energy gap of the Si-doped BNNT was more pronounced. The lipophilicity calculations indicated that the pure, Si- and Al-doped BNNTs are better candidates for increasing the efficiency of TEPA drug. It has been predicted that the Si-doped BNNT may be a promising drug delivery agent.

Keywords TEPA · BN/C nanotubes · Doping · Adsorption · DFT

1 Introduction

Carbon nanotubes (CNTs) have drawn great interests among scientific and engineering communities because of their marvelous shape, high stability and excellent conductivity since their innovation in 1991 [1–5]. Their illustrious mechanical and electronic properties have introduced them

as inspirational materials for recent applications such as fuel storage materials, energy capacitors and nanoelectronic devices [6, 7]. Low dispersion levels of carbon nanotube in polar liquids can be attributed to their hydrophobic-hydrophobic interactions which is a competitive task for their applications in nanoscale devices. For example, this special interaction of the CNTs is an important aspect for the significant increase in electrical and thermal conductivities of liquid suspensions and polymer composites. Many studies on the construction of functional carbon nanotube composites were achieved because of their extremely high Young's modulus [8], flexibility [9], electrical and thermal conductivity [10], large aspect ratio (typically ca. 300–1000), bending strength and chemical inertness. For example, the complexation of the CNTs with different molecules and structures, particularly oligonucleotides and proteins have been investigated inside [11] and outside [12, 13] of the nanotubes with their activities and immunological properties being retained [14, 15]. Their mechanical features, along with relatively low density [16], make the CNTs suitable candidates for weight-efficient structures and so they are intended to be the ultimate reinforcements in elastomer composites.

Several studies on different physicochemical aspects were focused on non-carbon nanotube structures. Amongst these structures, tubules made up of boron-nitride nanotubes

✉ Nafiseh Abdolahi
n_abdolahi2002@yahoo.com

✉ Alireza Soltani
Alireza.soltani46@yahoo.com; alireza.soltani@goums.ac.ir

¹ Biotechnology Research Center, Tabriz University of Medical Sciences, Tabriz, Iran

² Students Research Committee, Tabriz University of Medical Sciences, Tabriz, Iran

³ Department of Chemistry, Payame Noor University (PNU), Tehran, Iran

⁴ Department of Chemistry and Biotechnology, Swinburne University of Technology, Hawthorn, VIC 3122, Australia

⁵ Golestan Rheumatology Research Center, Golestan University of Medical Science, Gorgan, Iran

⁶ Department of Chemical Engineering, Xiamen University Malaysia, Jalan Sunsuria, Bandar Sunsuria, Selangor Darul Ehsan, 43900 Sepang, Malaysia

(BNNTs) were of great importance [17, 18]. BNNTs are structurally similar to their carbon-based counterparts and have many unique properties. For example, BNNTs have been introduced as a capable tool for the adsorption of compounds relevant to biomedical applications due to their high amount of binding energy [19, 20]. Unlike CNTs, BNNTs are wide bandgap semiconductors, insensitive to chirality and tube diameter which offer greater applications in electronic devices and sensors [21, 22]. Recent observations demonstrated that BNNTs could be non-cytotoxic, implying that they may emerge as novel biocompatible ingredients for therapeutic, biomedical or diagnostic applications [23, 24]. There have been many reports on the adsorption of drug molecules on different nanostructures with their applications [25–28]. For example, Kia and co-workers have shown the interaction of aminolevulinic acid (5-ALA) on the SWCNTs, C₆₀, and C₂₄ through density functional theory (DFT) calculations. They indicated that the adsorption of 5-ALA on these carbon nanostructures is mainly electrostatic in nature [29]. The structure and electronic properties of BNNTs functionalized with isoniazid drug molecule were studied by Sai-kiya and co-workers via DFT studies [30]. They found that the adsorption of isoniazid on the surfaces of (5, 5) and (10, 0) BNNTs are -0.649 and -0.738 eV, respectively.

TEPA (N, N', N''-triethylenephosphoramidate) is an alkylating agent that belongs to a family of pentavalent phosphorus compounds containing aziridinyl moieties that have been applied against various solid tumors as an active antiproliferative agent [31, 32]. TEPA is very unstable for clinical use because of its low lipophilicity (Log P = -0.62) whereas the more stable and lipophilic sulfur-substituted compound, Thiotepa (N, N', N''-triethylenethiophosphoramidate) was utilized clinically for more than 30 years (Log P = 0.57). However, the main disadvantage of the latter drug therapy is the high absorption level of this drug into the bloodstream which can result in bone marrow depression, leading to leukopenia, thrombocytopenia and anemia [33–35]. TEPA is the proposed metabolite of the alkylating anticancer agent Thiotepa, first represented in 1960 [36]. This anticancer system is metabolized in the liver after oxidative desulfuration by the action of the cytochrome P450 enzyme system and, most commonly used in the treatment of breast and bladder papillary cancer [34, 37, 38]. TEPA has a half-life of 2–7 times longer than that of the Thiotepa and is assumed to participate significantly in its antineoplastic activity [39, 40]. In addition, TEPA can be further metabolized non-enzymatically to monochlorotepa that has an alkylating activity significantly lower than that of TEPA [40]. This metabolite detected in the urine of patients treated with Thiotepa and may also be based on the chemical destruction of TEPA.

Concerning the advantages of TEPA over Thiotepa and the side effects of Thiotepa, it is necessary to find new

possible ways of using TEPA in the human body. In previous reports, studies have indicated that the increase in the lipophilicity of TEPA molecule increases the drug activity [33–35]. Therefore, the adsorption of TEPA on the CNTs and BNNTs were studied using DFT calculations to investigate the changes in lipophilicity and its stability for its utilization in the human body. The potentials of TEPA for drug delivery via nanotubes were also investigated in this work.

2 Computational Methods

First-principles computations for TEPA molecule interacted with the pristine, Al- and Si-doped (5, 5) CNTs and BNNTs have been performed using Gaussian 03 package [41] at the level of DFT with B3LYP/6-31G** level of the theory [42, 43]. For a weakly interacting system, dispersion forces become significant. Therefore, accurate estimates of binding energies are calculated via dispersion corrected functional. For this purpose, the adsorption energies have been investigated using M06-2X/6-31G** level of the theory [44, 45]. The adsorption energies (E_{ad}) of the TEPA molecule on the nanotubes were computed using the following equations:

$$E_{ad} = E_{TEPA/CNT} - [E_{CNT} + E_{TEPA}] \quad (1)$$

$$E_{ad} = E_{TEPA/Al-CNT} - [E_{Al-CNT} + E_{TEPA}] \quad (2)$$

$$E_{ad} = E_{TEPA/Si-CNT} - [E_{Si-CNT} + E_{TEPA}] \quad (3)$$

$$E_{ad} = E_{TEPA/BNNT} - [E_{BNNT} + E_{TEPA}] \quad (4)$$

$$E_{ad} = E_{TEPA/Al-BNNT} - [E_{Al-BNNT} + E_{TEPA}] \quad (5)$$

$$E_{ad} = E_{TEPA/Si-BNNT} - [E_{Si-BNNT} + E_{TEPA}] \quad (6)$$

where $E_{TEPA/CNT}$, $E_{TEPA/Al-CNT}$, $E_{TEPA/Si-CNT}$, $E_{TEPA/BNNT}$, $E_{TEPA/Al-BNNT}$ and $E_{TEPA/Si-BNNT}$ are the total energies of the CNT, Al-CNT, Si-CNT, BNNT, Al-BNNT and Si-BNNT interacted with TEPA molecule. E_{TEPA} , E_{CNT} , E_{Al-CNT} , E_{Si-CNT} , E_{BNNT} , $E_{Al-BNNT}$ and $E_{Si-BNNT}$ are the total energies of the lone TEPA, CNT, Al-CNT, Si-CNT, BNNT, Al-BNNT and Si-BNNT, respectively.

Physical and chemical properties of these adsorption systems were analyzed using the quantum molecular descriptors. The descriptors were defined by the following equations:

$$\mu = -\frac{I + A}{2} \quad (7)$$

$$\chi = -\mu \quad (8)$$

$$\eta = \frac{I - A}{2} \quad (9)$$

$$S = \frac{1}{2\eta} \quad (10)$$

$$\omega = \frac{\mu^2}{2\eta} \quad (11)$$

where ionization potential ($-E_{\text{HOMO}}$) and electron affinity ($-E_{\text{LUMO}}$) of a molecule were indicated as I and A respectively. Based on Koopmans' approximation, I and A can be expressed as $-E_{\text{HOMO}}$ and $-E_{\text{LUMO}}$ respectively. μ and χ are chemical potential and electronegativity. Equation (9) expresses the global hardness (η) according to the Koopmans' theorem. Softness (S) and electrophilicity index (ω) are specified using the Eqs. (10) and (11), respectively [46, 47]. The log P values were computed using ALOGPS 2.1 software in web service www.vclab.org, to predict their lipophilicities.

3 Results and Discussion

Figure 1 shows the molecular electrostatic potential (MEP) plot of the pristine TEPA molecule. As in this figure, the partial negative charges are mainly localized over the oxygen atom as oxygen has the highest electronegativity ($\chi = 3.5$) within the molecule as compared with nitrogen ($\chi = 3.0$)

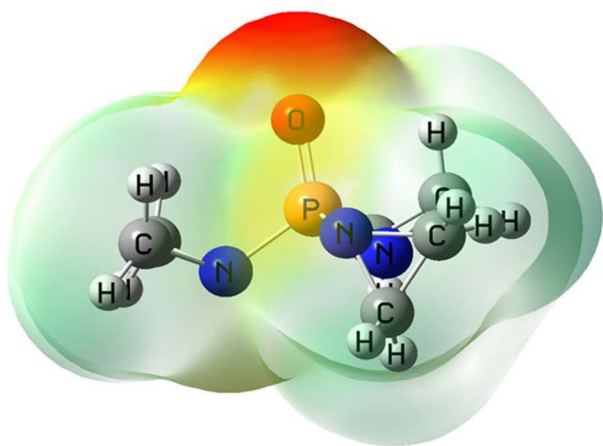


Fig. 1 Computed electrostatic potentials on the molecular surfaces of a bare TEPA molecule. (The color scheme for MEP surface is red-electron rich or partially negative charge; blue-electron deficient or partially positive charge; light blue-slightly electron deficient region; yellow-slightly electron rich region, respectively) (Color figure online)

and phosphorus ($\chi = 2.2$) atoms. The partial negative charge region hence becomes a favorable site for interaction with electron withdrawing and positive parts of the nanotubes. Herein, we discussed the optimized structures and geometry parameters of the pristine, Al- and Si-doped (5, 5) CNTs and BNNTs in the interaction with the TEPA molecule (Figs. 2 and 3). When one TEPA molecule is adsorbed toward the (5, 5) BNNT, the length of B–N bonds of this complex was slightly increased from 1.45 Å in the pristine nanotube to 1.46 Å. During the adsorption, the interaction of boron with oxygen causes the boron atoms in BNNT to have additional partial covalent bond. The bond addition will alter its default sp^2 -hybridization with three other nitrogen atoms in BNNT into a quasi sp^3 -hybridization as seen by the displacement of boron atom from the BNNT surface. This boron displacement is seen through the lengthen B–N bond and the non-zero dipole moment value (5.33 Debye) of TEPA/(5,5) BNNT due to the broken symmetry of BNNT structure which initially has zero dipole moment (DM).

The interaction of TEPA over BNNT (Tables 1 and 2) results in a weak interaction with the adsorption energies of -0.007 using the B3LYP and -0.292 eV using the M06-2X functional. With the comparison of the results obtained using the two applied functionals, it can be deduced that dispersion has a critical role in the TEPA adsorption over the pristine BNNT [48]. In addition, the calculated charge transfer analysis in the TEPA/(5, 5) BNNT complex is about 0.029 and 0.028 electrons at the B3LYP and M06-2X functionals, respectively. Furthermore, we used the Al- and Si-doped (5, 5) BNNTs for the adsorption of TEPA drug. For doping, a boron atom of BNNT is replaced with a Si or Al atom. The bond lengths were then measured and found to be 1.76 and 1.73 Å for N–Al and N–Si, respectively. After the optimization at the M06-2X functional and at the B3LYP functional, N–Al and N–Si bonds were measured to be 1.79 and 1.75 Å, respectively. The bond length calculated using the B3LYP functional is 1.83 Å for N–Al bond as reported by Soltani et al. [49]. The DM value for pristine Si-doped (5, 5) BNNT was calculated as 0.19 Debye, while the DM value of TEPA/Si-doped (5, 5) BNNT was about 4.61 Debye on M06-2X functional. These results indicate an increase in polarization after TEPA adsorption. For a better understanding of the adsorption properties of TEPA molecule attached to Si-doped (5, 5) BNNT, the charge analysis data were studied. It was found that charge transfer from the TEPA molecule to the Si-doped (5, 5) BNNT was about 0.069 and 0.058 electrons at the B3LYP and M06-2X functionals, respectively, implying insignificant charge transfer between TEPA molecule and Si-doped (5, 5) BNNT.

Adsorption energies for TEPA adsorption on Si-doped BNNT were calculated to be -0.209 eV and -0.574 eV in the B3LYP and M06-2X functionals, respectively. The nearest distances between TEPA and Si-doped BNNTs at

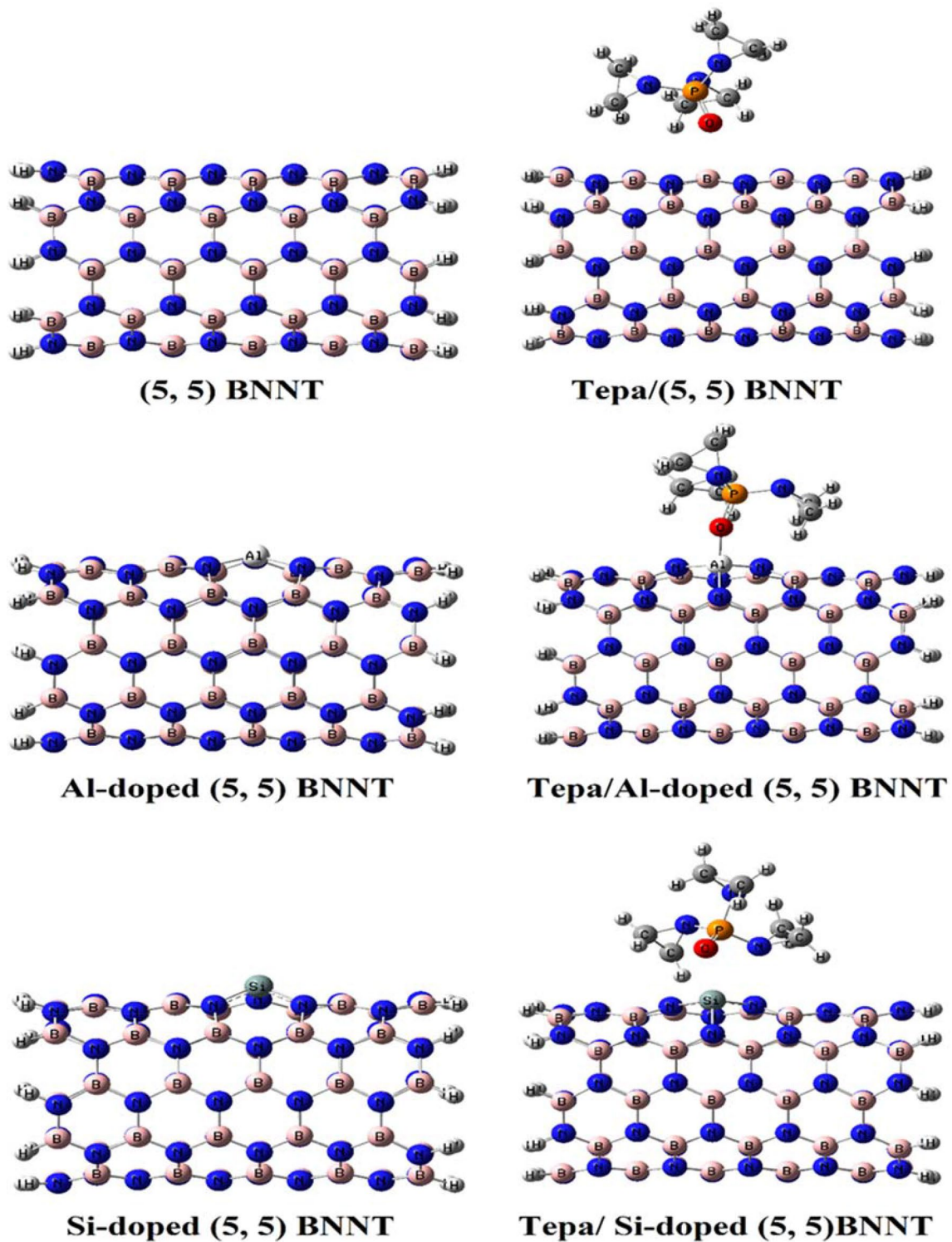


Fig. 2 Optimized configurations for the BNNT, TEPA/BNNT, Al-doped BNNT, TEPA/Al-doped BNNT, Si-doped BNNT and TEPA/Si-doped BNNT at the M06-2X method

the B3LYP and M06-2X methods were obtained as 2.77 and 2.89 Å, respectively. Adsorption energies for TEPA adsorption on Al-doped BNNT were calculated to be -2.110 eV

and -2.530 eV with the nearest adsorbent-adsorbate distances of 1.83 and 1.82 Å via B3LYP and M06-2X functionals, respectively. Comparisons of the TEPA adsorption

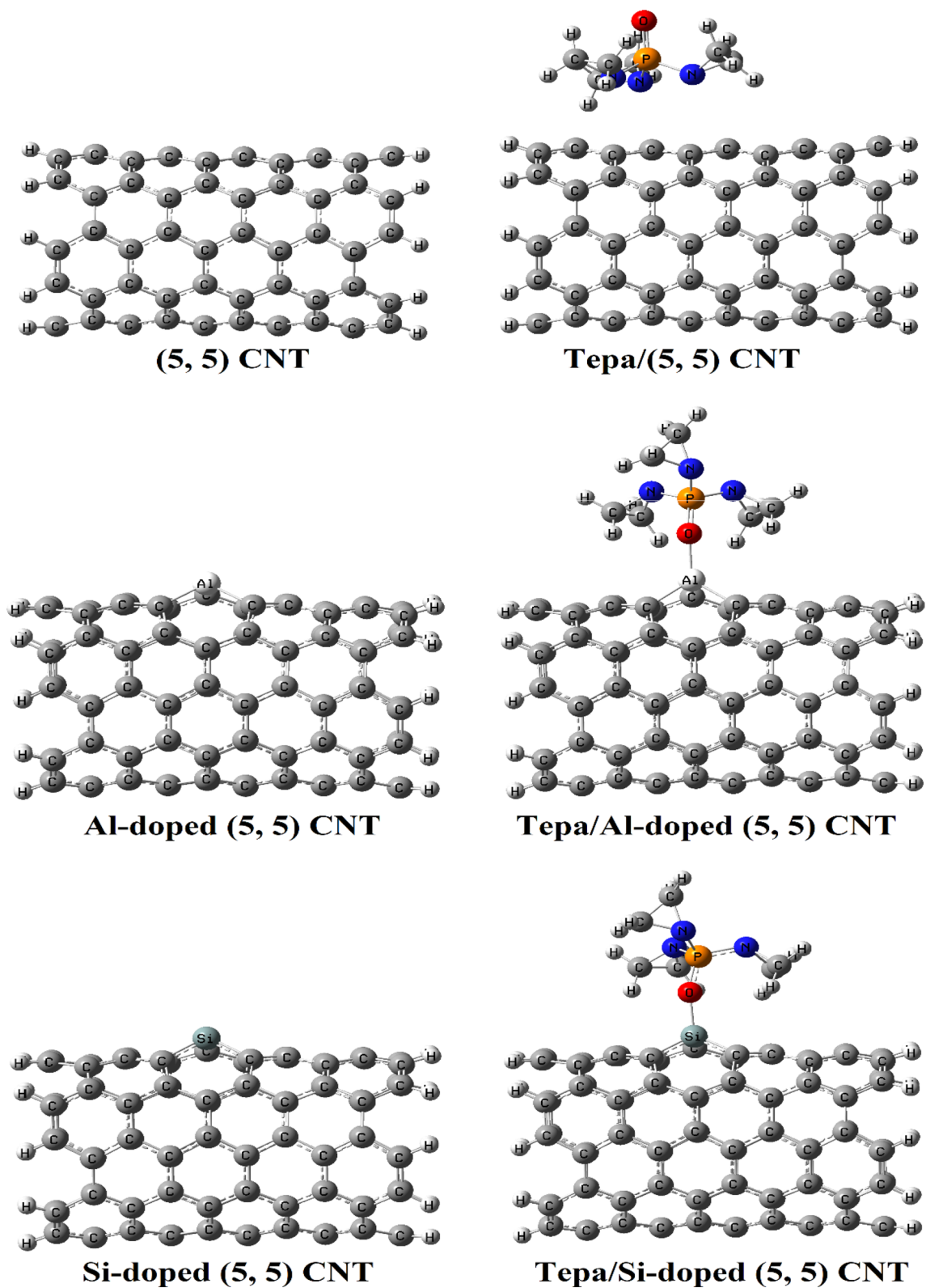


Fig. 3 Optimized configurations for the CNT, TEPA/CNT, Al-doped CNT, TEPA/Al-doped CNT, Si-doped CNT and TEPA/Si-doped CNT at the M06-2X method

Table 1 Adsorption energy, E_{HOMO} and E_{LUMO} , band gap (E_g), energy of Fermi level (E_F) and dipole moment (Debye) of pristine nanotubes and adsorbed TEPA on these nanostructures in B3LYP method

Entry	TEPA	(5,5) CNT	Al-CNT	Si-CNT	(5,5) BNNT	Al-BNNT	Si-BNNT	TEPA/(5,5) CNT	TEPA/(5,5) CNT	TEPA/Si-CNT	TEPA/(5, 5) BNNT	TEPA/Al-BNNT	TEPA/Si-BNNT
E_{ad}	-	-	-	-	-	-	-	0.001	-1.93	-1.09	-0.007	-2.11	-0.209
${}^aQ_T(\text{e})$	-	-	-	-	-	-	-	0.006	0.316	0.378	0.029	0.331	0.069
HOMO	6.61	-4.32	-4.11	-4.35	-6.44	-6.41	-5.32	-4.26	-3.67	-3.67	-6.28	-5.96	-4.93
E_F	-2.33	-3.48	-3.33	-3.57	-3.27	-3.85	-2.72	-3.41	-2.90	-2.90	-3.13	-2.87	-2.45
LUMO	1.94	-2.63	-2.56	-2.80	-0.10	-1.28	-0.12	-2.56	-2.12	-2.14	0.01	0.23	0.04
E_g	8.55	1.70	1.55	1.55	6.35	5.13	5.20	1.70	1.55	1.53	6.28	6.19	4.97
DM	2.37	0.00	0.40	0.82	0.02	1.39	0.14	0.90	12.36	14.72	5.61	12.24	5.06

The parameters are in units of eV

aQ is defined as the average of total charge on the molecule

Table 2 Adsorption energy, E_{HOMO} and E_{LUMO} , energy gap (E_g), energy of Fermi level (E_F) and dipole moment (Debye) of pristine nanotubes and adsorbed TEPA on these nanostructures in M06-2X method

Entry	TEPA	(5,5) CNT	Al-CNT	Si-CNT	(5,5) BNNT	Al-BNNT	Si-BNNT	TEPA/(5,5) CNT	TEPA/(5,5) CNT	TEPA/Si-CNT	TEPA/(5, 5) BNNT	TEPA/Al-BNNT	TEPA/Si-BNNT
E_{ad}	-	-	-	-	-	-	-	-0.432	-2.463	-1.816	-0.292	-2.530	-0.574
${}^aQ_T(\text{e})$	-	-	-	-	-	-	-	0.015	0.307	0.380	0.028	0.330	0.058
HOMO	3.07	-5.23	-5.01	-5.27	-7.96	-7.93	-6.61	-5.22	-4.57	-4.61	-7.80	-7.56	-6.27
E_F	-2.69	-3.74	-3.54	-3.79	-3.52	-4.22	-2.86	-3.67	-3.12	-3.14	-3.40	-3.19	-2.63
LUMO	-8.46	-2.18	-2.08	-2.31	0.92	-0.51	0.90	-2.11	-1.68	-1.68	0.99	1.18	1.02
E_g	11.54	3.10	2.92	2.96	8.88	7.41	7.51	3.11	2.89	2.93	8.79	8.74	7.29
DM	2.42	0.00	0.87	0.16	0.00	1.38	0.19	0.99	11.82	14.12	5.33	11.06	4.61

The parameters are in units of eV

aQ is defined as the average of total charge on the molecule

energies on the Si- and Al-doped BNNT indicate that dispersion calculation is a significant factor in the adsorption calculations [48]. The higher adsorption energies of Al-doped BNNT is attributed to its ability as Lewis acid site in accepting a lone pair of electrons from oxygen atom at its $3p$ empty orbital. Based on B3LYP and M06-2X functionals, 0.331 and 0.330 electrons were respectively transferred from the TEPA to the Al-doped BNNT after the adsorption. In a study, the adsorption values of propargylamine-based sulfonamide over the pristine, Si, and Al-doped BN nanotubes were calculated to be -0.13 , -0.65 , and -1.25 eV, respectively [49]. Their results indicated that Si and Al-doped BN nanotubes have stronger interaction with the sulfonamide than that of the pristine BN nanotube. Compared to the pure (5, 5) BNNT, the adsorption of the TEPA bindings on the Si- and Al-doped BNNTs were known to be stronger compared to that of the bare BNNT which may be related to the electronic properties and reactivity of the Al and Si atoms in the outer sidewalls of the BNNT.

In Fig. 3, we calculated the interaction of a TEPA drug molecule with the pristine, Si- and Al-doped (5, 5) CNT using the B3LYP and M06-2X functionals. For the TEPA/CNT complex, the adsorption energy and distance are -0.432 eV and 2.85 Å, respectively at the M06-2X functional. The results indicate that the interaction of TEPA with CNT was stronger than that of the BNNT. The dipole moment value increased from zero Debye in the pure CNT to 0.99 Debye in the TEPA/CNT complex. The C-Si and C-Al bonds in the pristine Si- and Al-doped CNTs were slightly increased from 1.78 to 1.85 Å to 1.79 and 1.91 Å after the adsorption processes, respectively at the M06-2X functional, which are in well accordance with the previous reports [50, 51]. The dipole moment value for TEPA drug molecule interacting with the Si- and Al-doped CNTs are 14.12 and 11.82 Debye, denoting an increase in dipole moment value after the adsorption process. Computed adsorption energies of TEPA/Si-doped CNT and TEPA/Al-doped CNT were -1.816 eV and -2.463 eV at the M06-2X functional (see Table 1), which explain the chemisorption of the drug towards the tubular wall of the Si- and Al-doped CNTs. The closest distances of the TEPA and Si- and Al-doped CNTs were 1.76 and 1.83 Å, and the charge transfers from the TEPA to the Si- and Al-doped CNTs were obtained to be 0.380 and 0.307 electron, respectively. The re-hybridization of dopant atoms from sp^2 to sp^3 may be the key factor for the chemisorption of TEPA on the Si- and Al-doped CNTs. Compared to the pure (5, 5) BNNT, the adsorption of the TEPA exhibits stronger bindings towards Si- and Al-doped CNTs.

In the next stage, we investigated the electronic energies of TEPA for the most stable adsorption configuration upon the CNTs and BNNTs. The energies of HOMO (the highest occupied molecular orbital) and LUMO (the lowest

unoccupied molecular orbital) were also investigated using DFT calculations. The HOMO orbitals in the pure, Si- and Al-doped BNNT complexes illustrate that the electrons are located upon the TEPA molecule, while the LUMO orbitals of these complexes are situated upon the B and N atoms of the tubes. The HOMO and LUMO of TEPA molecule interacting with the pure, Si- and Al-doped CNTs are located upon the C-C orbitals (see Figs. 4 and 5). The HOMO and LUMO orbitals are often associated with the ability to donate and accept an electron, respectively [49]. The obtained values of HOMO and LUMO energies of the studied complexes are presented in Tables 1 and 2.

The obtained values of energy gap (E_g) for pristine CNT and BNNT are 1.70 and 6.35 eV on the B3LYP functional and 3.10 and 8.88 eV on the M06-2X functional, respectively, which is in a good agreement with the previous reports [52, 53]. The E_g of the BNNT slightly reduces from 8.88 eV in the pristine tube to 8.79 eV in TEPA-adsorbed form at the M06-2X functional, so that the energy gap differs negligibly between the two species. The value of E_g after adsorption process was increased from 7.41 eV in Al-doped BNNT to 8.74 eV in TEPA/Al-doped BNNT. This event shows that although the Al-doping significantly improves the interaction between TEPA and BNNT, it largely reduces the electronic sensitivity of the systems [54–57]. However, the result for the Si-doped BNNT was slightly different in which the E_g of the Si-doped BNNT decreased after TEPA adsorption. This decrement in the E_g exponentially enhances the electrical conductivity of the whole adsorbent-adsorbate complex that can be converted to an electrical signal for a better detection of the TEPA drug by the Si-BNNT [58]. However, unlike the Al-doping, the Si-doping enhances the sensitivity of the BN nanotube towards the TEPA drug. The energy band gap values of the pure, Si-, and Al-doped CNTs were unchanged after the adsorption of TEPA as the LUMOs at C-C orbitals were not involved as the chemisorption site for TEPA. This result suggests the adsorption of TEPA has no significant effect on the electronic properties of the pure, Si- and Al-doped (5, 5) CNTs.

The total density of states (TDOS) and projected density of state (PDOS) plots of the pure BNNT, Al-doped BNNT, Si-doped BNNT, pure CNT, Al-doped CNT and Si-doped CNT interacting with the TEPA molecule in the states A, B, C, D, E, and F are depicted in Fig. 6. PDOS plots of first (tube) and the second (drug) fragments are shown as red and blue colors of the specified complexes. The vertical lines indicate the E_F position and edge of the valence band. According to Fig. 6 for all the calculated states, the new states favor increasing the band gap of the Al- and Si-doped BNNTs and CNTs. Different states of the PDOS exactly represent a dependency of the electronic structure of the interaction systems to the spectral adsorption position and orientation of the TEPA interaction with

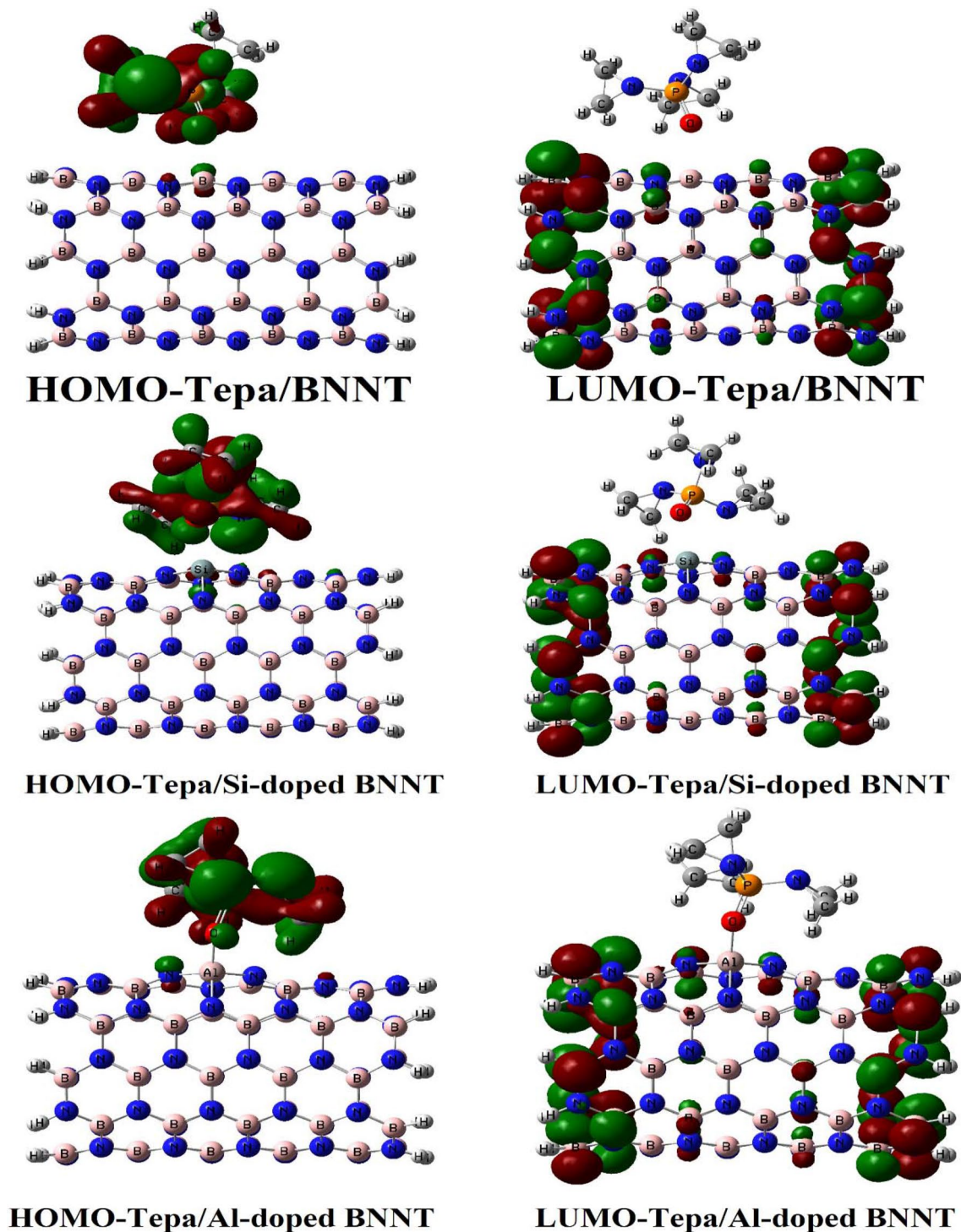


Fig. 4 Molecular orbitals of the HOMO and LUMO on the pristine, Si- and Al-doped (5, 5) BNNT loaded with TEPA at the M06-2X method

the pure and doped BNNTs and CNTs. Figure 5 shows significant changes in the energy of the donor state in **C**, **D**, **E**, and **F** configurations. By the PDOS plots, it can be understood that the HOMO and LUMO states of the doped BNNTs and CNTs states were significantly altered upon

their interactions with TEPA, suggesting that the TEPA drug was chemically adsorbed (chemisorption) upon the outer surfaces of the doped BNNTs and CNTs that consequently result in a charge transfer between the doped nanotubes and TEPA drug.

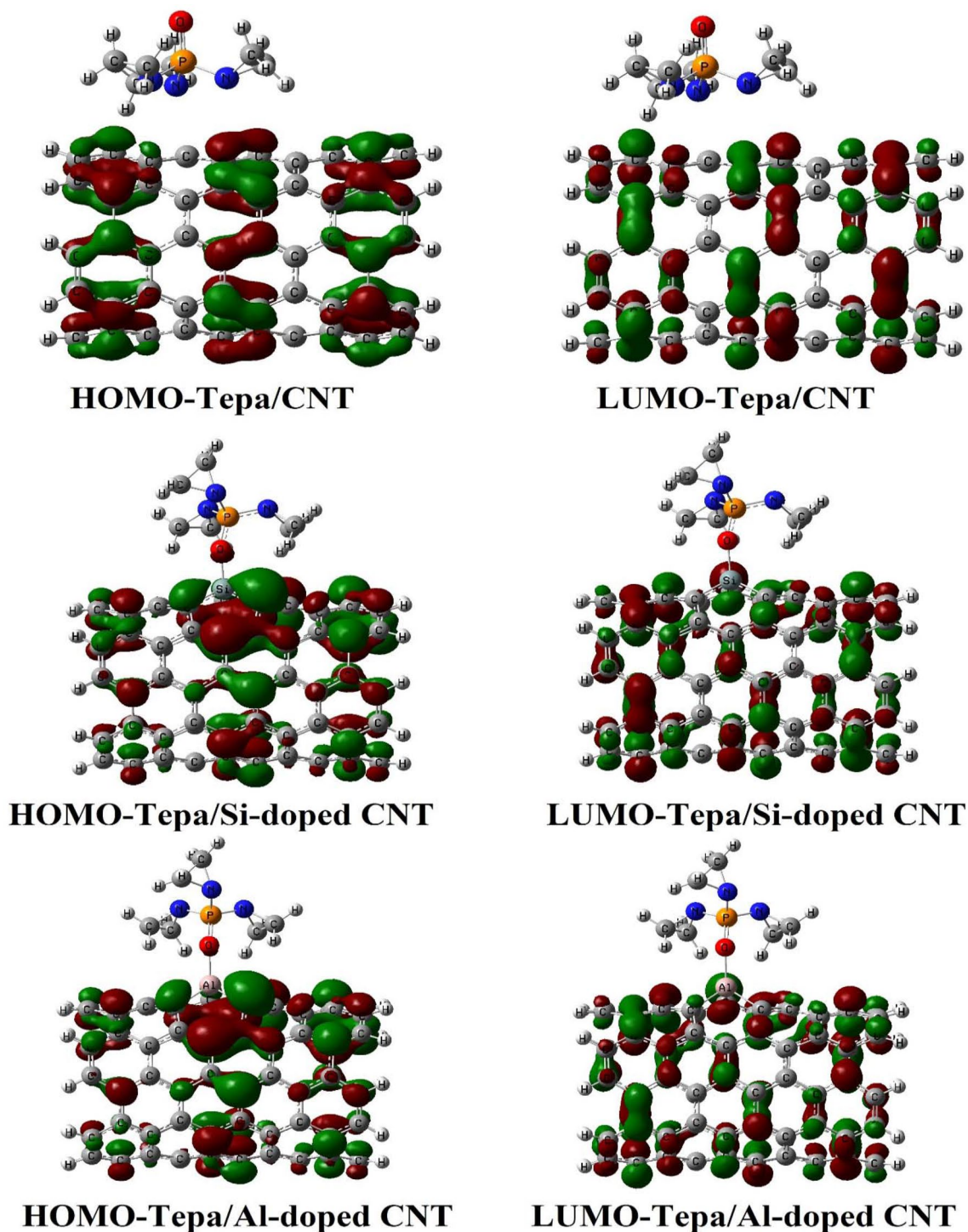


Fig. 5 Molecular orbitals of the HOMO and LUMO on the pristine, Si- and Al-doped (5, 5) CNT loaded with TEPA at the M06-2X method

Figure 7 shows the electron density (ED) maps of Al- and Si-doped BNNTs and CNTs interacting with the TEPA molecule. The charge transfers occurring from the TEPA to doped BNNTs and CNTs near the adsorption sites were mainly due to the strong chemical interactions in the states C, D, E and F [59, 60]. The covalent bonding relates to the

overlapping of molecular orbitals and electrons primarily agglomerated at the center of the bond as shown in the states C, D, E and F. As it is shown in the Fig. 7, the electron charge density distribution is obviously centralized around the Al and oxygen atoms of the complex indicating a significant overlapped charge density which is in agreement with

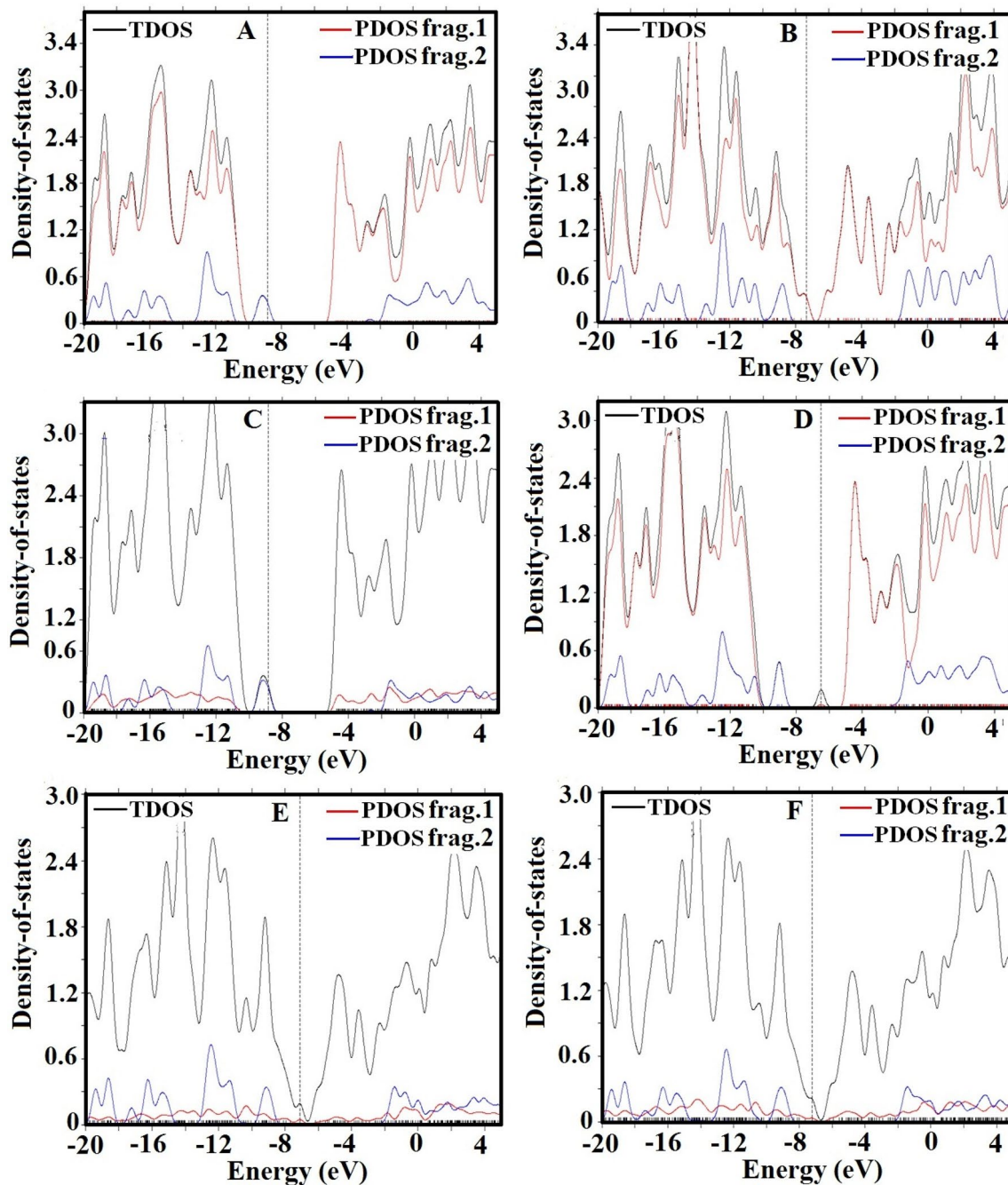


Fig. 6 PDOS plots of TEPA interacting with BNNT (a), CNT (b), Al-doped BNNT (c), Si-doped BNNT (d), Al-doped CNT (e), and Si-doped CNT (f)

the covalent interaction between drug and doped nanotubes, leading to the chemical adsorption and high binding energy of the TEPA drug towards the doped BNNTs and CNTs. For TEPA/Si-doped BNNT system (State E), the oxygen atom partially overlapped with Si atom in Si-doped BNNT. The

oxygen atom chemisorption was also noted to be facilitated by the partial interaction of B atom as B atom has similar role with Al atom as Lewis acid site due to its one empty valence orbital. In comparisons with other adsorption systems with direct interaction of O and Al atoms, these partial

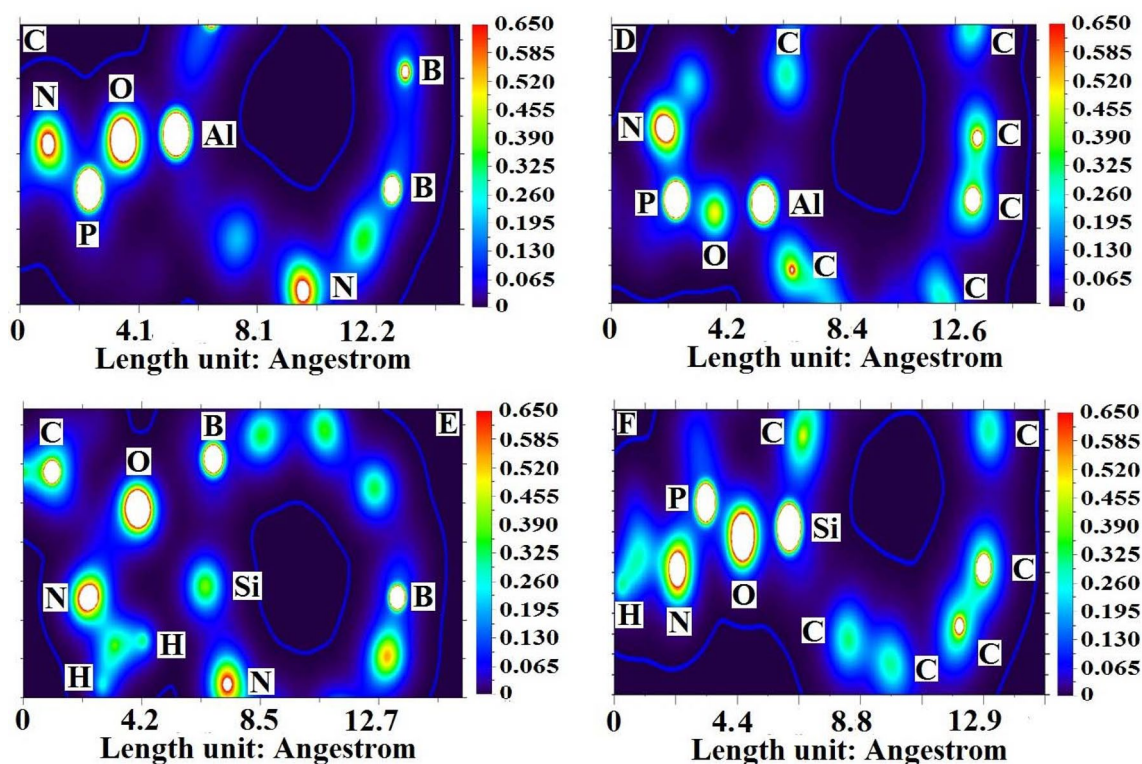


Fig. 7 ED plots of TEPA interacting with Al-doped BNNT (c), Al-doped CNT (d), Si-doped BNNT (e) and Si-doped CNT (f)

interactions in TEPA/Si-doped BNNT system would certainly have a weaker binding energy as evident by its smaller adsorption energy. Electron deficient hydrogen atoms of N-CH₃ group in TEPA were also noted to form hydrogen bonds via their interactions with the lone pair electrons of nitrogen atom in the Si-doped BNNT.

The quantum molecular descriptors (QMDs) for the studied adsorption configurations at the M06-2X/6-31G* level of theory are shown in Table 3. The values of η for the (5,5) CNT, Al-CNT, Si-CNT, (5,5) BNNT and Si-BNNT were negligibly changed by the adsorption of TEPA. These results are in good agreement with the E_g trend of the nanotubes on TEPA adsorption. TEPA/Si-BNNT is more interested in changes under electrical field conditions compared to the pristine nanotube [61]. The values of A and I for TEPA/Si-BNNT, TEPA/Al-BNNT, TEPA/Si-CNT and TEPA/Al-CNT were noted to be smaller than that of their adsorption configurations using pristine BNNT and CNT. This indicates

the higher stability of the Si- and Al-doped complexes as compared to the pristine nanotube complexes. The values of ω and χ were noted to be reduced after TEPA adsorption, indicating a decline in the reactivity of systems or it could be interpreted as the adsorption system reaching a more stable state in resisting chemical changes [62].

To evaluate the lipophilicity of the generated complexes, their log P values were computed using ALOGPS 2.1 software to predict their stability and solubility in the body (Table 4). It has been pointed out that lipophilicity is an important factor for biochemical, pharmacological and environmental processes in quantitative structure–activity relationship (QSAR) studies [63, 64]. Studies on TEPA-adsorbent systems indicated that the increase in the lipophilicity ($0 \ll \log P \ll 2$) could increase the efficiency of this drug [33]. The log P values reveal that the pure, Si-, and Al-doped CNTs can be the most toxic molecules with the greatest log P values (≈ 7.2). These results also render the CNT based adsorbents not to be in the proper range of increasing the

Table 3 Quantum molecular descriptors for TEPA interacted with nanotubes in M06-2X method

Entry	TEPA	(5,5) CNT	Al-CNT	Si-CNT	(5,5) BNNT	Al-BNNT	Si-BNNT	TEPA/(5,5) CNT	TEPA/Al-CNT	TEPA/Si-CNT	TEPA/(5,5) BNNT	TEPA/Al-BNNT	TEPA/Si-BNNT
I (eV)	8.46	5.29	5.01	5.27	7.96	7.93	6.61	5.22	4.57	4.61	7.80	7.56	6.27
A (eV)	-3.08	2.18	2.08	2.31	-0.92	0.51	-0.90	2.11	1.68	1.68	-0.99	-1.18	-1.02
η (eV)	5.77	1.55	1.46	1.48	4.44	3.71	3.75	1.56	1.45	1.46	4.40	4.37	3.65
μ (eV)	-2.69	-3.74	-3.54	-3.79	-3.52	-4.22	-2.86	-3.67	-3.12	-3.15	-3.40	-3.19	-2.63
S (eV)	2.88	0.78	0.73	0.74	2.22	1.85	1.88	0.78	0.72	0.73	2.20	2.18	1.82
ω (eV)	0.63	4.50	4.29	4.85	1.39	2.40	1.09	4.32	3.37	3.38	1.32	1.16	0.95
χ (eV)	2.69	3.74	3.54	3.79	3.52	4.22	2.86	3.67	3.12	3.15	3.40	3.19	2.63

Ionization potential (I), vertical electron affinity (A), hardness (η), chemical potential (μ), softness (S), electrophilicity (ω) and electronegativity (χ)

drug efficiency. On the other hand, the lipophilicity of the TEPA/(5, 5) BNNT, TEPA/Si-BNNT and TEPA/Al-BNNT were higher as compared to TEPA and remain in the optimum range of $0 \ll \log P \ll 2$. Thus, this is a good indicator of the potential of these carriers to be used in the body for the increase in the efficiency of TEPA molecule inside the body.

4 Conclusions

Herein this study, we reported on the adsorption, electronic and structural properties of the pure, Si-, and Al-doped (5, 5) BNNTs and CNTs with a TEPA drug molecule using DFT calculations. It was found that TEPA has a weak adsorption energy with the pure BNNT and CNT. The adsorption energy values of TEPA drug in the interaction with the Si-doped CNT, Al-doped CNT, Si-doped BNNT and Al-doped BNNT were calculated to be -1.81 , -2.46 , -0.57 and -2.53 eV, respectively. Charge transfer calculation reveals the occurrence of charge transfer from TEPA drug molecule to the applied adsorbents. Although the Si- and Al-doped CNTs and Al-doped BNNT are great adsorbents, the sensitivity of TEPA drug is understood to be more on the Si-doped BNNT compared to other studied adsorbents. The lipophilicity calculations indicated that the BNNTs are better candidates, as compared to CNTs, for increasing the efficiency of TEPA drug. The calculated results revealed that the Si-doped BNNT can be a reliable adsorbent to be used as a TEPA drug delivery carrier and can increase the efficiency of TEPA molecule in the body.

Table 4 log P values for TEPA and TEPA adsorption complexes

Entry	TEPA	TEPA/(5,5) CNT	TEPA/Al-CNT	TEPA/Si-CNT	TEPA/(5,5) BNNT	TEPA/Al-BNNT	TEPA/Si-BNNT
log P	-0.57	7.27	7.24	7.26	1.15	1.48	1.27
	-0.62 [35]						

Acknowledgements We thank Tabriz University of Medical Sciences for providing partial support of the instrumental analysis facilities. The authors want to thank the clinical Research Development Unit (CRDU), Sayad Shirazi Hospital, Golestan University of Medical Sciences, Gorgan, Iran.

Compliance with Ethical Standards

Conflict of interest The authors declare that they have no conflict of interest.

References

- S. Iijima, Nature **354**, 56 (1991)
- I. Deretzi, A. La Magna, Physica E **40**, 2333 (2008)
- B. Bellafi, S. Haddad, I. Sfar, S. Charfi-Kaddour, Phys. B **404**, 524 (2009)
- K. Tsukagoshi, N. Yoneya, S. Uryu, Y. Aoyagi, A. Kanda, Y. Ootuka, B. Alphenaar, Phys. B **323**, 107 (2002)
- J. Beheshtian, A.A. Peyghan, Z. Bagheri, J. Mol. Model. **19**, 391 (2013)
- M. Terrones, W.K. Hsu, H.W. Kroto, D.R. Walton, *Fullerenes and Related Structures* (Springer, New York, 1999), pp. 189–234
- M.S. Dresselhaus, G. Dresselhaus, P.C. Eklund (Academic press, New York, 1996)
- T. Uchida, S. Kumar, J. Appl. Polym. Sci. **98**, 985 (2005)
- C. Cooper, R. Young, M. Halsall, Composites Part A **32**, 401 (2001)
- S.J. Tans, A.R. Verschuere, C. Dekker, Nature **393**, 49 (1998)
- J.J. Davis, M.L. Green, H.A.O. Hill, Y.C. Leung, P.J. Sadler, J. Sloan, A.V. Xavier, S.C. Tsang, Inorg. Chim. Acta **272**, 261 (1998)
- F. Balavoine, P. Schultz, C. Richard, V. Mallouh, T.W. Ebbesen, C. Mioskowski, Angew. Chem. Int. Ed. **38**, 1912 (1999)
- Z. Guo, P.J. Sadler, S.C. Tsang, Adv. Mater. **10**, 701 (1998)
- A. Bianco, M. Prato, Adv. Mater. **15**, 1765 (2003)
- D. Pantarotto, C.D. Partidos, R. Graff, J. Hoebeke, J.-P. Briand, M. Prato, A. Bianco, J. Am. Chem. Soc. **125**, 6160 (2003)
- G. Gao, T. Cagin, W.A. Goddard, Nanotechnology **9**, 184 (1998)
- L. Li, C.P. Li, Y. Chen, Physica E **40**, 2513 (2008)
- V.S.K. Choutipalli, V. Subramanian, Phys. Chem. Chem. Phys. **19**, 15377 (2017)
- C.M. Chang, A.F. Jalbout, Thin Solid Films **518**, 2070 (2010)
- M. Mirzaei, M. Yousefi, Superlattices Microstruct. **55**, 1 (2013)
- G. Guo, J. Lin, Phys. Rev. B **71**, 165402 (2005)
- M. Solimannejad, M. Noormohammadbeigi, J. Iran. Chem. Soc. **14**, 471 (2017)
- X. Chen, P. Wu, M. Rousseas, D. Okawa, Z. Gartner, A. Zettl, C.R. Bertozzi, J. Am. Chem. Soc. **131**, 890 (2009)
- G. Ciofani, S. Danti, D. D'Alessandro, S. Moscato, A. Menciassi, Biochem. Biophys. Res. Commun. **394**, 405 (2010)
- H. Chen, B. Wang, D. Gao, M. Guan, L. Zheng, H. Ouyang, Z. Chai, Y. Zhao, W. Feng, Small **9**, 2735 (2013)
- G. Ciofani, V. Raffa, J. Yu, Y. Chen, Y. Obata, S. Takeoka, A. Menciassi, A. Cuschieri, Curr. Nanosci. **5**, 33 (2009)
- G. Ciofani, Expert Opin. Drug Deliv. **7**, 889 (2010)
- A.K. Attia, N.F. Abo-Talib, M.H. Tammam, Adv. Pharm. Bull. **7**, 151 (2017)
- M. Kia, M. Golzar, K. Mahjoub, A. Soltani, Superlattices Microstruct. **62**, 251 (2013)
- N. Saikia, S.K. Pati, R.C. Deka, Appl. Nanosci. **2**, 389 (2012)
- K. Sugiura, C.C. Stock, M.M. Sugiura, Cancer Res. **15**, 38 (1955)
- A. Craig, H. Jackson, Br. J. Pharmacol. **10**, 321 (1955)
- S.M. Musser, S.S. Pan, M.J. Egorin, D.J. Kyle, P.S. Callery, Chem. Res. Toxicol. **5**, 95 (1992)
- D.A. Williams, T.L. Lemke, *Foye's Principles of Medicinal Chemistry, 2002* (Lippincott and Wilkins, Philadelphia, 2007), p. 5
- G. Sosnovsky, J. Lukszo, M. Konieczny, K. Purgstaller, F. Laib, J. Pharm. Sci. **83**, 982 (1994)
- L. Mellett, L. Woods, Cancer Res. **20**, 524 (1960)
- T. Chang, G. Chen, D.J. Waxman, J. Pharmacol. Exp. Ther. **274**, 270 (1995)
- S. Ng, D.J. Waxman, Cancer Res. **50**, 464 (1990)
- N.A. Cohen, M.J. Egorin, S.W. Snyder, B. Ashar, B.E. Wietharn, S. Pan, D.D. Ross, J. Hilton, Cancer Res. **51**, 4360 (1991)
- P.J. O'Dwyer, F. LaCreta, P.F. Engstrom, R. Peter, L. Tartaglia, D. Cole, S. Litwin, J. DeVito, D. Poplack, R.J. DeLap, Cancer Res. **51**, 3171 (1991)
- M. Frisch, G. Trucks, H. Schlegel, G. Scuseria, M. Robb, J. Cheeseman, J. Montgomery Jr., T. Vreven, K. Kudin, J. Burant, *Gaussian 03, Revision B. 05, Pople, in* (Gaussian, Inc, Pittsburgh PA, 2003)
- W. Hehre, L. Radom, J. Pople, P.V.R. Schleyer, *Ab Initio Molecular Orbital Theory* (Wiley, New York, 1986)
- P. Geerlings, F. De Proft, W. Langenaeker, Chem. Rev. **103**, 1793 (2003)
- Y. Zhao, D.G. Truhlar, Theor. Chem. Acc. **120**, 215 (2008)
- A.S. Rad, K. Ayub, J. Mol. Liq. **238**, 303 (2017)
- A.S. Rad, Appl. Surf. Sci. **357**, 1217 (2015)
- A. Soltani, M.B. Javan, M.S. Hoseininezhad-Namin, N. Tajabor, E.T. Lemeski, F. Pourarian, Synth. Met. **234**, 1 (2017)
- M. Walker, A.J. Harvey, A. Sen, C.E. Dessent, J. Phys. Chem. A **117**, 12590 (2013)
- N. Saikia, R.C. Deka, Chem. Phys. **500**, 65 (2010)
- R. Bian, J. Zhao, H. Fu, J. Mol. Model **19**, 1667 (2013)
- E. Rahmanifar, M. Yoosofian, H. Karimi-Maleh, Synth. Met. **221**, 242 (2016)
- M.S. Hoseininezhad-Namin, P. Pargolghasemi, S. Alimohammadi, A.S. Rad, L. Taqavi, Physica E **90**, 204 (2017)
- A. Soltani, M.T. Baei, E.T. Lemeski, S. Kaveh, H. Balakheyli, J. Phys. Chem. Solids **86**, 57 (2015)
- A. Soltani, S. Ghafouri Raz, V. Joveini Rezaei, A. Dehno Khalaji, M. Savar, Appl. Surf. Sci. **263**, 619 (2012)
- A. Soltani, N. Ahmadian, Y. Kanani, A. Dehnokhalaji, H. Mighani, Appl. Surf. Sci. **258**, 9536 (2012)
- A. Ahmadi Peyghan, A. Soltani, A.A. Pahlevani, Y. Kanani, S. Khajeh, Appl. Surf. Sci. **270**, 25 (2013)

57. S.F. Rastegar, A. Ahmadi Peyghan, N.L. Hadipour, *Appl. Surf. Sci.* **265**, 412 (2013)
58. Q. Yuan, Y.-P. Zhao, L. Li, T. Wang, *J. Phys. Chem. C* **113**, 6107 (2009)
59. A. Soltani, M. Bezi Javan, M.T. Baei, Z. Azmoodeh, *J. Alloy. Compd.* **735**, 2148 (2018)
60. N. Abdolahi, M. Aghaei, A. Soltani, Z. Azmoodeh, H. Balakheyli, F. Heidari, *Spectrochim. Acta Part A* **204**, 348 (2018)
61. A.S. Rad, K. Ayub, *J. Alloys Compd.* **672**, 161 (2016)
62. Z. Mahdaviifar, N. Abbasi, *Physica E* **56**, 268 (2014)
63. R. Wang, Y. Fu, L. Lai, *J. Chem. Inf. Comput. Sci.* **37**, 615 (1997)
64. P. Pargolghasemi, M. Saleh Hoseininezhad-Namin, A. Parchehbaf Jadid, *Curr. Comput. Aided Drug Des.* **13**, 249 (2017)

Publisher's Note Springer Nature remains neutral with regard to jurisdictional claims in published maps and institutional affiliations.